Two-dimensional hydrogen-bonded assemblies: the influence of sterics and competitive hydrogen bonding on the structures of guanidinium arenesulfonate networks

Victoria A. Russell and Michael D. Ward*

Department of Chemical Engineering and Materials Science, University of Minnesota, Amundson Hall, 421 Washington Ave. SE, Minneapolis, MN 55455, USA

Guanidinium and organosulfonate ions self-assemble into crystalline lattices described by robust two-dimensional hydrogen-bonded networks with the general formula $[C(NH_2)_3]^+RSO_3^-$. These networks, which typically have quasihexagonal symmetry due to favourable hydrogen bonding between six guanidinium proton donors and six sulfonate electron lone pair acceptors, assemble in the third dimension by stacking in a manner which maximizes van der Waals interactions between R groups. The steric requirements of the R groups dictate whether this assembly results in interdigitated bilayer stacking in which all the R groups are orientated to one side of a given sheet or interdigitated single layer stacking in which R groups are orientated to both sides of a given hydrogen-bonded sheet. The two-dimensional network tolerates very different steric requirements of the R groups due to the ability to form either of these stacking motifs and to the inherent flexibility of the hydrogen-bonded network about one-dimensional hydrogen-bonding 'hinges'. This flexibility allows the sheets to pucker in order to accommodate steric strain between R groups within the layers. We describe here the influence of substituents on the R groups whose steric and hydrogen bonding capacity influence the puckering of the two-dimensional guanidinium sulfonate network. In particular, we examine the X-ray crystal structures of the guanidinium salts of ferrocenesulfonate and methyl- and nitro-substituted benzenesulfonates. The retention of the hydrogen-bonding motif in spite of steric and hydrogen bonding interference by the R group substituents illustrates the robustness of the guanidinium sulfonate network. However, additional competing hydrogen bonding and sterics influence the crystal packing, and in the case of multiple substituents on the R groups, these factors may disrupt the guanidinium sulfonate network. Overall, this work demonstrates that the use of robust two-dimensional supramolecular modules can reduce the crystal engineering problem to the last remaining dimension, which can simplify the design of functional molecular materials.

Introduction

Crucial to the design and synthesis of molecular materials is a thorough understanding, and ultimately control, of the assembly of constituent molecules into the supramolecular motif that defines the solid state structure. It is instructive to consider the constituent molecules of a material as the fundamental building blocks of the solid state. The formation of ordered solid-state networks with a desired arrangement and dimensionality relies on an appropriate 'topological director', that is, a module having a well-defined functional group that can recognize complementary functional groups on other like molecules (homomeric assembly) or different molecules (heteromeric assembly). A crucial property of a director is its ability to participate in intermolecular interactions which are strong and highly directional relative to competing ones. Formation of extended networks also requires 'polyvalent' modules, that is, molecules having more than one bonding functionality. These capabilities are provided by molecules containing hydrogen bonding functionalities.

Several examples of ordered, extended hydrogen bonding networks have been reported that illustrate the important influence of this interaction on directing the organization of molecules in the crystallization of solid-state materials. These reports have demonstrated that the local supramolecular organization about each module can be predicted with reasonable confidence based on molecular topology. Flat molecules having one-dimensional hydrogen-bonding topologies form 'ribbon' or 'tape' networks,[1–5] while tetrahedral-like hydrogen-bonding topologies have afforded diamondoid networks.[6–10] However, control of packing in three dimensions can be elusive owing to the contribution of numerous intermolecular interactions in the crystal, many of which are nondirectional, resulting in a multiplicity of structural possibilities. Furthermore, most of the aforementioned systems either do not provide for the systematic introduction of ancillary molecular functionality that is required for the synthesis of functional materials, or are susceptible to dramatic changes in crystal packing upon such changes. A reasonable strategy for surmounting these obstacles is to use *robust* supramolecular 'modules'[11,12] or 'synthons',[13] where robust is defined as the ability of the module to maintain its dimensionality and general structural features upon changes in ancillary functional groups or other molecular species in the lattice. Robust *n*-dimensional modules can reduce the crystal engineering problem to 3-*n* dimensions, thereby simplifying materials design.

Recently, we reported molecular layered materials based on a two-dimensional hydrogen-bonded (HB) network composed of guanidinium cations (**G**) and the sulfonate groups of alkane- and arene-substituted monosulfonate anions (**S**).[14–17] The topological equivalence of the guanidinium ions and sulfonate groups and strong (guanidinium)N—H , O(sulfonate) hydrogen bonds favoured the formation of quasihexagonal two-dimensional **GS** networks in over 30 different crystalline phases containing various sulfonate functionalities (Fig. 1). All the hydrogen bonding capacity is fulfilled within this network, which is important in forming robust networks. The networks assembled in the third dimension *via* van der Waals interactions between sulfonate R groups extending from the **GS** sheets, either as densely packed bilayers or continuous stacks of interdigitated single layers. The pervasiveness of the **GS** sheets was attributed to their ability to form 'accordion' or 'pleated' sheets by puckering about (guanidinium)N—H , O(sulfonate) HB 'hinges' joining adjacent one-dimensional hydrogen-bonded ribbons. This puckering, which can be defined by inter-ribbon dihedral angles of $h_{IR} < 180°$, enables the sheets to adapt to the steric demands of different R groups. In a few cases these steric demands were also accommodated by the formation of a shifted ribbon HB motif. Although considered to be less optimal than the quasihexagonal motif because of the loss of one strong hydrogen bond, two-dimensional sheet formation in the shifted motif was enforced by the one remaining strong inter-ribbon hydrogen bond. Such motifs offer unique opportunities for new layered materials based on the **GS** network

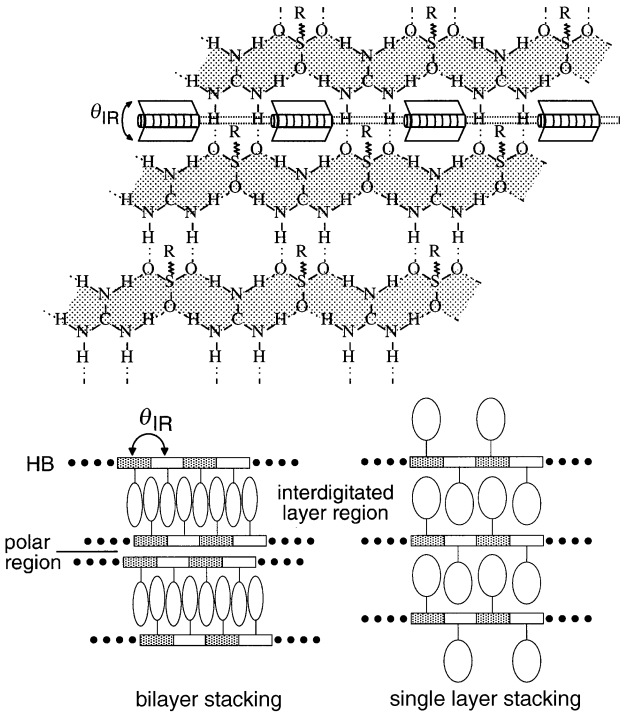

Fig. 1 (Top) Schematic representation of the sheet-like HB networks formed from guanidinium cations and alkane- and arene-substituted monosulfonates and disulfonates. The most commonly observed network is quasihexagonal, in which every sulfonate oxygen atom is hydrogen bonded to two guanidinium protons (typical $d_{O\cdots H}=2.0$ Å) so that all HB capacity is fulfilled. These sheets can be considered as assembling from one-dimensional HB ribbons (shaded) *via* hydrogen bonds. In some compounds these hydrogen bonds behave as hinges, resulting in a pleated **GS** network that can adapt to the steric requirements of the R groups. The inter-ribbon puckering angle is described by h_{IR}. (Bottom) Schematic representations of layered materials synthesized from guanidinium cations and alkane- and arene-substituted monosulfonates, as viewed along the long axis of the HB ribbons contained in the nominally planar **GS** networks. The white and shaded rectangles represent the narrow edge of the ribbons. Bilayer motifs (left) are observed for R groups which are small enough to allow interdigitation of R groups in the non-polar region separating the **GS** sheets. If the alkane or arene groups are too large, the R groups of adjacent ribbons are orientated to opposite sides of each sheet, which provides room for interdigitation and the continuous single layer stacking of the **GS** sheets (right). The sheets can adapt further to the steric requirements of the R groups in either layering motif by puckering about (guanidinium)N-H , O(sulfonate) HB 'hinges' between adjacent ribbons (h_{IR}).

with optical, magnetic, or conducting properties that will depend upon the choice of molecules in the region spanning the layers. However, a precise understanding of the influence of R group substituents, specifically the proximity of these substituents to and their ability to interact with the HB network, is required for rational design of such materials. This prompted us to examine systematically the influence of substituents on arenesulfonates whose steric and hydrogen bonding capacity influence the puckering of the two-dimensional **GS** network. The layered motif is retained in spite of steric interference and competing hydrogen bonding interactions in a majority of cases, illustrating the robustness of this network. Most importantly, our results demonstrate that the use of robust two-dimensional supramolecular modules can reduce the crystal engineering problem to the last remaining dimension.

Results and Discussion

Substituent sterics and hydrogen bonding

The occurrence of either the interdigitated bilayer or the continuously stacked single layer motif can be predicted, at least as a first approximation, from the gross steric requirements of the R group extending from the **GS** sheets (Fig. 2). If the R group is described by either spheres or cylinders it can be shown that interdigitation in a bilayer motif is possible only if the diameter of the R group, as viewed normal to the hydrogen-bonded sheet, is less than $d_{S\text{-}S}/\sqrt{3}$, where $d_{S\text{-}S}$ is the centre-to-centre distance between nearest sulfonate residues (typically *ca.* 7.5 Å). If the diameter exceeds this value of *ca.* 4.4 Å, interdigitation is not possible in the bilayer motif. Rather, the networks resort to the continuously stacked single layer motif in which the interdigitation is possible because the R groups of adjacent ribbons are orientated to opposite sides of the **GS** sheet. Previously, we illustrated several examples that conformed to this model (although in most cases the sulfonate residue is not rigorously cylindrical). For example, guanidinium naphthalene-2-sulfonate, (**G**)(**1**), assembles into the bilayer stacking motif (with $h_{IR}=146°$), whereas the sterically more demanding naphthalene-1-sulfonate homologue (**G**)(**2**) assembles into the single layer stacking motif (with $h_{IR}=77°$).[14] The effect of steric demand is also evident in the structure of the guanidinium salt of ferrocenesulfonate (**3**), which exhibits the continuously stacked single layer stacking motif (Fig. 3). Although the steric 'footprint' of **3** (43 Å^2) is larger than that of **2** (31 Å^2), the puckering of the **GS** sheet is less severe. This reflects the need for the network to pucker more in (**G**)(**2**) in order to recover the dense packing lost by forming the single layer motif. The dense packing in (**G**)(**2**) is achieved through p–p stacking interactions between neighbouring naphthyl residues (distance between neighbouring ring planes *ca.* 4.1 Å). In contrast, the cross-sectional area of the ferrocene residue is comparable to the molecular area of a guanidinium sulfonate

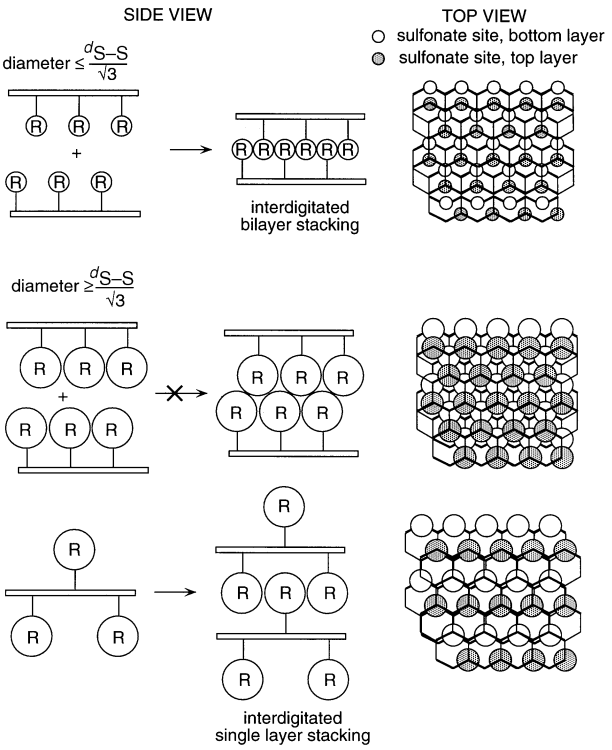

Fig. 2 Schematic representation illustrating the steric influence of the R group on the layering motif in guanidinium sulfonate salts. Interdigitation of R groups all arranged on the same side of the hydrogen-bonded sheet is possible if the R group projected diameter $< d_{S\text{-}S}/\sqrt{3}$ (*ca.* 4.4 Å) where $d_{S\text{-}S}$ is the distance between nearest sulfonate groups. This results in the bilayer structure (top). If the diameter $> d_{S\text{-}S}/\sqrt{3}$, interdigitation is not possible (centre) and the single layer motif (bottom), in which R groups on adjacent ribbons are orientated to opposite sides, is formed as this allows interdigitation and efficient packing between the hydrogen-bonded sheets.

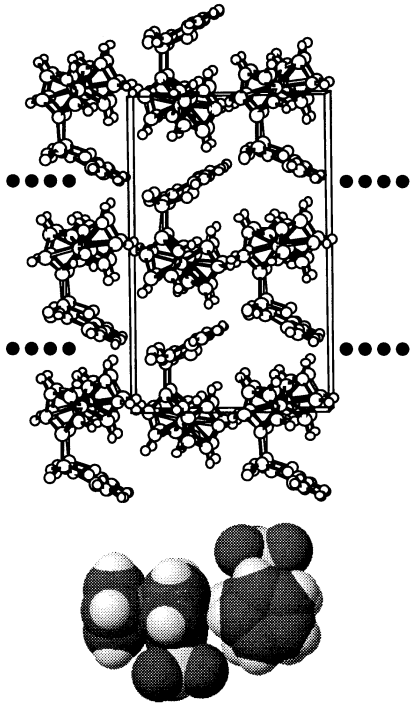

(G)(3)

Fig. 3 (Top) Crystal structure of guanidinium ferrocenesulfonate (**G**)(**3**), as viewed along the hydrogen-bonded ribbon direction, which extends out of the plane of the page. This view illustrates the segregation of the non-polar ferrocene-containing regions and the polar hydrogen-bonding regions into a puckered interdigitated single layer motif. The filled circles denote the hydrogen-bonded quasihexagonal **GS** sheet. (Bottom) Space-filling representation of the packing of two adjacent ferrocene residues contained within the (100) galleries of (**G**)(**3**). The C–H dipole of one of the residues projects into the centre of the cyclopentadiene ring of the neighbouring ferrocene, suggesting Cd^{-}–Hd^{+} , p-electron interactions.

unit (*ca.* 45 Å^2), therefore requiring less puckering than (**G**)(**2**) to recover lost packing density. The C—H dipole of each ferrocene projects into the centre of the cyclopentadiene ring of a neighbouring ferrocene, suggesting a role for Cd^{-}—Hd^{+} , p-electron interactions in the ordering of these residues (see Fig. 3). The ferrocene containing phase introduces redox centres into 'galleries' between the robust two-dimensional layers, suggesting interesting possibilities for charge trapping and electron transport. The structure of this salt resembles recently reported materials which are based on two-dimensional zirconium phosphonate (ZrP) networks with redox centres within the galleries defined by ZrP layers.[19–21]

While the aforementioned model has been useful in the design and synthesis of over 30 crystalline **GS** salts containing the two-dimensional hydrogen-bonded network,[12] it does not address the more subtle effects of positional substitution. Proximity of functional groups to the **GS** sheet may perturb significantly the planarity of these networks, and in severe cases, may actually prohibit formation of the two-dimensional network. If these functional groups are hydrogen-bond donors or acceptors, competition with complementary sites of the **GS** sheet may perturb the hydrogen bonding and geometry of the **GS** network. Previously, we discovered that the guanidinium salt of *p*-carboxybenzenesulfonate (**4**) did not form layered networks because of hydrogen-bonding competition of the carboxylic acid group for guanidinium proton donor and sulfonate oxygen acceptor sites.[15] However, the two-dimensional layer structure was preserved for guanidinium salts of benzenesulfonates with weaker hydrogen-bonding substituents such as the phenolic group in *p*-hydroxybenzenesulfonate (**5**) and the nitro group in *p*-nitrobenzenesulfonate (**6**), whose structures exhibited the single layer motif with substantial corrugation of the **GS** sheet ($h_{IR} = 51°$ and 72°, respectively). In contrast, the guanidinium salt of *p*-toluenesulfonate (**7**), which has a size similar to that of **5** and **6** but no hydrogen bonding capability, exhibited the bilayer motif with modest puckering ($h_{IR} = 151°$). This demonstrated that the layering motif adopted by these materials was influenced by both steric and hydrogen bonding effects. Although the bilayer motif should have been accessible to **5** and **6** based on steric effects alone, a highly puckered single layer motif was formed owing to modest hydrogen bonding competition by the hydroxy and nitro groups for the sulfonate oxygens and guanidinium protons, respectively.

In order to elucidate the relative contributions of steric and hydrogen-bonding competition effects from substituents forced to be in close proximity to the **GS** sheet, we have examined the guanidinium salts of various *ortho*- and *meta*-substituted methyl- and nitro-benzenesulfonates (**8–16**). An *ortho* substituent may sterically block the sulfonate oxygen acceptor sites by hindering the approach of the potential guanidinium donor (Scheme 1). The oxygen atoms of the nitro groups, as hydrogen-bonding acceptors, may compete for the guanidinium protons in the **GS** sheet. Nitro groups generally are not strong hydrogen-bond acceptors, particularly when compared to the sulfonate oxygen atoms, suggesting that the perturbation of the **GS** network may not be so severe that its formation is prohibited. Our previous observation that the *p*-nitrobenzenesulfonate compound (**G**)(**6**) possesses the quasihexagonal **GS** network, in contrast to (**G**)(**4**) which contains the stronger hydrogen-bonding carboxylic acid group, supports this contention. Investigation of the *ortho*- and *meta*-substituted phases allows comparison between residues with identical volumes but with substituents in different positions. The conformational freedom of the *ortho* substituents also can provide steric relief and minimize the perturbation of the **GS** sheet.

Synthesis of guanidinium arenesulfonates

Guanidinium salts of variously substituted methyl- and nitrobenzenesulfonates were prepared by slow evaporation crystallization techniques. Several of these compounds appeared to form unstable solvated crystalline phases, as evidenced by the physical transformation of transparent crystals to opaque solids soon after their removal from the mother liquor. Low temperature broad endotherms observed by differential scanning calorimetry (DSC) of samples characterized immediately after their removal from solution also suggested the loss of solvent from the crystals, and IR spectroscopy confirmed the presence of solvent molecules in the solids. IR spectroscopy also revealed that several of these phases did not contain the desired quasihexagonal HB sheet motif. Consequently, we pursued characterization of phases which were stable under ambient conditions and/or that contained the two-dimensional HB motif. Although unstable phases were sometimes isolated, stable, high quality crystals suitable for single crystal X-ray diffraction were obtained readily for most of the substituted arenesulfonates depicted above. Experimental details of the X-ray structural determinations are given in Table 1. All of the phases described here for which crystal structures have been determined exhibit typical molecular geometries, including the guanidinium ions and $-SO_3$ groups. Therefore, detailed descriptions of the molecular structures are not presented here.

Methyl-substituted sulfonates

Crystal structures were determined for guanidinium salts of toluene-3-sulfonate (**G**)(**9**), and mesitylenesulfonate (**G**)(**11**), which crystallize in orthorhombic space group *Pnma* (Fig. 4). The salt (**G**)(**9**) crystallizes with quasihexagonal **GS** sheets which are extremely puckered ($h_{IR} = 88°$) and assemble into the

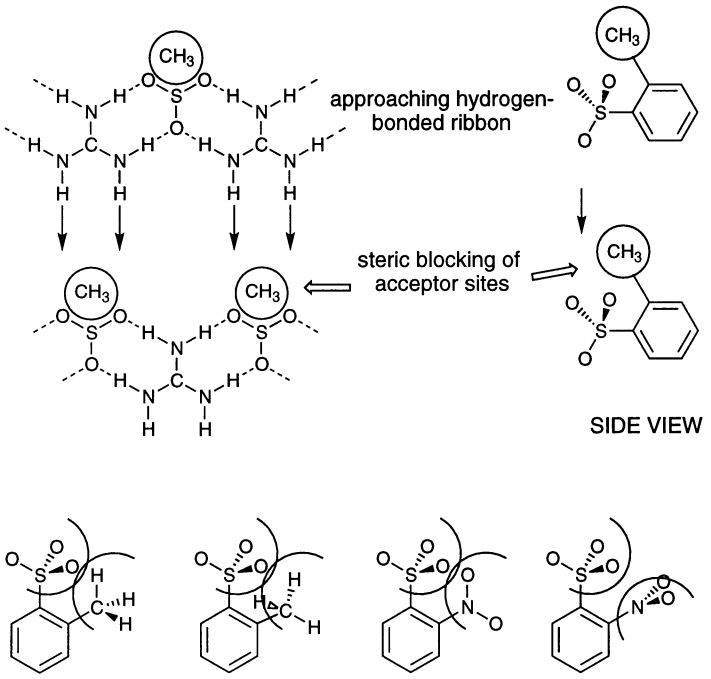

Scheme 1

interdigitated single layer stacking motif. The structural details of the layering motifs are summarized for these compounds, and for the other layered materials described below, in Table 2. The packing of (**G**)(**9**) into a puckered single layer rather than a bilayer motif is somewhat surprising, as the *para*-tolyl compound (**G**)(**7**) crystallizes into a bilayer structure with a herringbone arrangement of adjacent arene rings within the bilayer galleries. The *meta*-methyl substituent does not block the approach of the guanidinium protons to the sulfonate acceptor sites, so a similar bilayer motif may be expected. However, the interactions between neighbouring inversion-related arene rings in the region between the **GS** sheets in (**G**)(**9**) appear to differ from the herringbone orientations observed in (**G**)(**7**) and other guanidinium arenesulfonates, with each methyl group in (**G**)(**9**) lying over the p-system of a neighbouring arene ring (see Fig. 4).

Highly puckered quasihexagonal **GS** sheets ($h_{IR} = 86°$) and the interdigitated single layer stacking motif also are observed in (**G**)(**11**). The presence of the quasihexagonal topology, in which all six sulfonate oxygen lone electron pairs participate in hydrogen bonding to the guanidinium protons with typical hydrogen bond distances, indicates that the *ortho* methyl substituents in (**G**)(**11**) do not prohibit the formation of this network. However, the mesitylenesulfonate ion does not exceed the steric limit of *ca.* 4.4 Å which is considered the threshold of stability for the interdigitated bilayer structure. Steric interference by the *ortho*-methyl substituents hinders coplanar approach of the hydrogen-bonded ribbons to form a two-dimensional sheet if the mesitylene groups are orientated to the same side of the HB sheet (see Scheme 1). Thus, the ribbons are forced to approach each other nearly orthogonally, with the mesitylene groups of neighbouring ribbons orientated to opposite sides of the hydrogen-bonding plane, resulting in substantial puckering. The nearly identical packing of (**G**)(**11**) and (**G**)(**9**) is reflected in the similarities of the *b* and *c* crystallographic lattice constants in these phases. The repeat distances parallel and perpendicular to the hydrogen bonding ribbon in the **GS** network, denoted as d_{rib} and $d_{\backslash rib}$, respectively, are nearly identical in (**G**)(**9**) and (**G**)(**11**). The stacking repeat distance, d_{stk}, is larger for (**G**)(**11**) than for (**G**)(**9**) due to the steric demand of the *para*-methyl substituent in (**G**)(**11**) ($d_{stk} = 8.71$ and 10.51 Å for (**G**)(**9**) and (**G**)(**11**), respectively). The arene–arene interactions in the organic region are best described as offset p-stacking interactions in both salts, whereas in the (**G**)(**7**) and other guanidinium arenesulfonate salts, herringbone motifs are present.

The crystal structures of the 2-methylbenzenesulfonate (toluene-2-sulfonate) (**G**)(**8**) and its 2,4-dimethylbenzenesulfonate homologue (**G**)(**10**) could not be determined because of poor crystal quality. In the case of (**G**)(**8**), the fine needles obtained were not large enough and attempts to crystallize an unsolvated form always led to opaque solids with poor crystallinity. Crystallographic data for (**G**)(**10**) could not be refined satisfactorily. However, the IR spectral features for (**G**)(**8**) and (**G**)(**10**), particularly in the $n_{N\text{-}H}$ region, are essentially identical to those of (**G**)(**9**), (**G**)(**11**) and (**G**)(**7**) (Fig. 5). Correlation of IR spectral data and X-ray crystal structures for over 30 **GS** salts in our laboratory has demonstrated that a particular absorption band profile in the $n_{N\text{-}H}$ region from 3500–3100 cm^{-1} (as in Fig. 5) is highly diagnostic of the quasihexagonal HB sheet motif. Consequently, we surmise from examination of the IR absorption band structures observed for the unsolvated forms of (**G**)(**8**) and (**G**)(**10**) that these compounds also form layered structures containing the quasihexagonal HB sheet.

Nitro-substituted sulfonates

Each guanidinium salt of the variously substituted nitrobenzenesulfonates, guanidinium 2-nitrobenzenesulfonate (**G**)(**12**), 3-nitrobenzenesulfonate (**G**)(**13**), 2,4-dinitrobenzenesulfonate (**G**)(**14**), 2,4-dinitrobenzenesulfonate monohydrate (**G**)(**14**)·$\mathbf{H_2O}$, and picrylsulfonate (**G**)(**15**) crystallizes in space group *P*1 with one ion pair per asymmetric unit. The nitro N—O bond geometries compare well with those determined from a search of the Cambridge Crystallographic Database, which revealed a mean $d_{N\text{-}O}$ of 1.217 ± 0.011 for 1116 aromatic nitro compounds.[18] The twisting of the *ortho* nitro groups out of the arene ring plane in compounds (**G**)(**12**), (**G**)(**14**), (**G**)(**14**)·H_2O and (**G**)(**15**) is 50–60°. In contrast, the *para* nitro group is nearly coplanar in (**G**)(**6**), (**G**)(**14**), (**G**)(**14**)·$\mathbf{H_2O}$ and (**G**)(**15**). A value of 16° is observed for the *meta* nitro group in (**G**)(**13**). The severe twisting of the *ortho*

Table 1 Crystallographic data for guanidinium sulfonates

compound	(G)(3)	(G)(9)	(G)(11)	(G)(12)	(G)(13)	(G)(14)	(G)(14)·H_2O	(G)(15)
formula	$C_{11}H_{15}N_3O_3SFe$	$C_8H_{13}N_3O_3S$	$C_{10}H_{17}N_3O_3S$	$C_7H_{10}N_4O_5S$	$C_7H_{10}N_4O_5S$	$C_7H_9N_5O_7S$	$C_7H_{11}N_5O_8S$	$C_7H_8N_6O_9S$
M_W	325.16	231.27	259.33	262.25	262.24	307.24	324.24	352.23
crystal size/mm^3	$0.67\times0.57\times0.05$	$0.57\times0.47\times0.27$	$0.50\times0.30\times0.08$	$0.50\times0.38\times0.25$	$0.60\times0.30\times0.25$	$0.55\times0.50\times0.42$	$0.55\times0.50\times0.42$	$0.55\times0.50\times0.42$
crystal system	orthorhombic	orthorhombic	orthorhombic	triclinic	triclinic	triclinic	triclinic	triclinic
space group	$Pna2_1$	$Pnma$	$Pnma$	$P1$	$P1$	$P1$	$P1$	$P1$
a/Å	17.160(6)	17.410(8)	21.021(2)	7.2416(8)	7.196(8)	7.761(3)	7.715(2)	7.782(6)
b/Å	7.693(4)	7.595(6)	7.5584(6)	7.5908(9)	7.628(6)	7.842(4)	8.314(4)	8.187(2)
c/Å	10.740(4)	8.613(4)	8.3710(6)	12.1475(14)	11.694(5)	11.591(3)	10.987(5)	10.813(2)
a (°)	90	90	90	88.257(2)	76.45(5)	97.87(3)	82.73(4)	100.83(2)
b (°)	90	90	90	78.135(2)	78.32(8)	95.33(3)	72.25(3)	92.32(4)
c (°)	90	90	90	62.150(1)	62.94(9)	118.32(4)	77.88(2)	99.20(6)
V/Å^3	1418(2)	1139(2)	1330.0(2)	576.12(11)	552(2)	605(1)	655(1)	666(1)
Z	4	4	4	2	2	2	2	2
D_{calc}/g cm^{-3}	1.523	1.349	1.295	1.512	1.577	1.686	1.645	1.756
F (000)	672	488	552	272	272	316	334	360
m (Mo-K_a) (cm^{-1})	12.09	2.64	2.45	2.98	2.97	2.97	2.84	2.93
T/°C	24	24	25	24	24	24	24	24
diffractometer type	Enraf-Nonius	Enraf-Nonius	Siemens	Siemens	Enraf-Nonius	Enraf-Nonius	Enraf-Nonius	Enraf-Nonius
scan mode	v	v	—	—	v-2h	v-2h	v	v-2h
scan speed (deg/min in v)	1.8–16.5	16.5	—	—	8.2	8.2	8.2–16.5	16.5
$2h_{max}$ (°)	52.0	47.9	48.2	48.2	56.0	55.9	55.9	63.9
range of *hkl*	$-21,\pm9,\pm13$	$\pm8,-9,\pm19$	-24 to $22,-4$ to $8,\pm9$	$\pm8,\pm8,-5$ to $+13$	$+9,\pm9,\pm14$	$\pm10,\pm10,\pm15$	$\pm10,\pm11,\pm14$	$\pm10,\pm11,\pm15$
no. refl. collected	4087	3727	5066	2470	5310	2989	3256	6019
no. unique refl.	2595	1077	1134	1742	2655	2919	3138	4613
R_{int}	0.054	0.048	0.045	0.0313	0.040	0.022	0.024	0.023
corrections applied[a]	abs, 2 ext	abs, 2 ext	abs	abs	abs, 2 ext	abs	abs, 2 ext	2 ext
R^b	0.045	0.060	0.050	0.0405	0.042	0.052	0.070	0.047
$R_w{}^b$	0.046	0.075	0.111	0.1052	0.055	0.056	0.067	0.058
D(r) e/Å^{-3}	0.39	0.94	0.154	0.281	0.42	0.47	0.46	0.48
no. indep refl obs $I>2s(I)$	1571	735	1134	1742	2287	2218	2018	3544
N_o/N_v	9.13	8.65	11.57	8.98	12.78	12.25	10.35	15.21
GOF	1.12	2.26	1.098	1.073	2.01	1.74	2.05	1.55

[a]All structures were corrected for Lorentz and polarization effects. abs = empirical absorption using DIFABS (N. Walker and D. Stuart, *Acta Crystallogr. Sect. A*, 1983, **39**, 158.); 2 ext = secondary extinction. [b]$R(F)=S||F_o|-|F_c||/S|F_o|$. [c]$R(wF)=[(Sw(|F_o|-|F_c|)^2/SwF_o^2)]^{1/2}$; $w=4F_o^2/s^2(F_o^2)$.

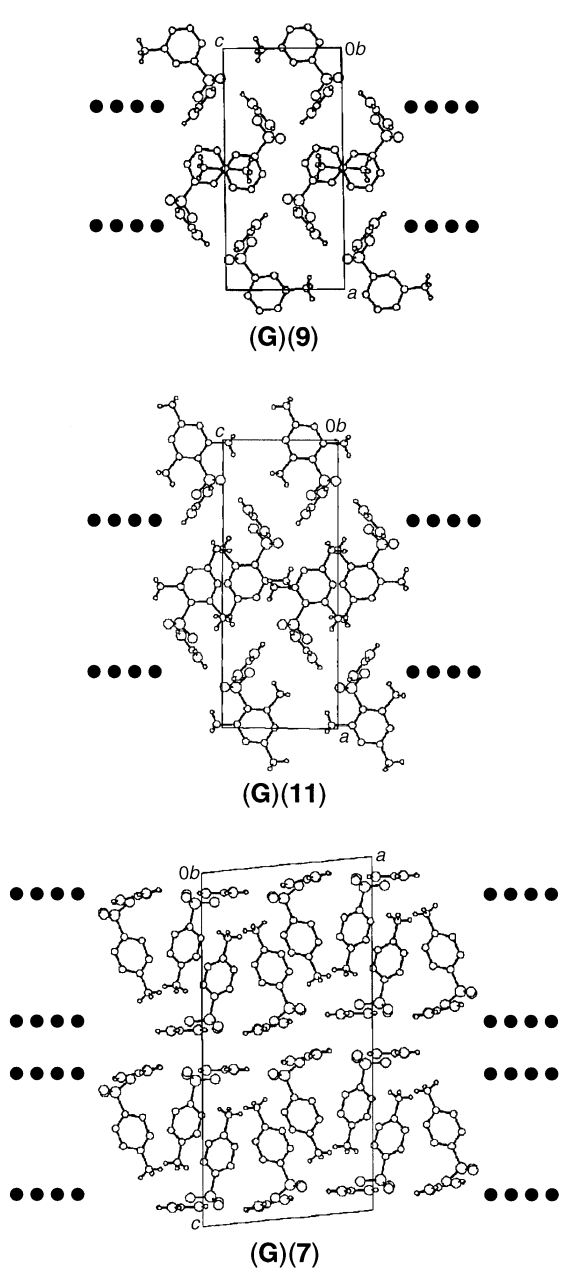

Fig. 4 Crystal structures of guanidinium toluene-3-sulfonate (**G**)(**9**), guanidinium mesitylenesulfonate (**G**)(**11**), and guanidinium toluene-4-sulfonate (**G**)(**7**) as viewed along the hydrogen-bonded ribbon direction, which extends out of the plane of the page. These views illustrate the segregation of the non-polar arene-containing regions and the polar hydrogen-bonding regions into bilayers for (**G**)(**7**), and severely puckered interdigitated single layers for (**G**)(**9**) and (**G**)(**11**). The filled circles denote the hydrogen-bonded quasihexagonal **GS** sheet.

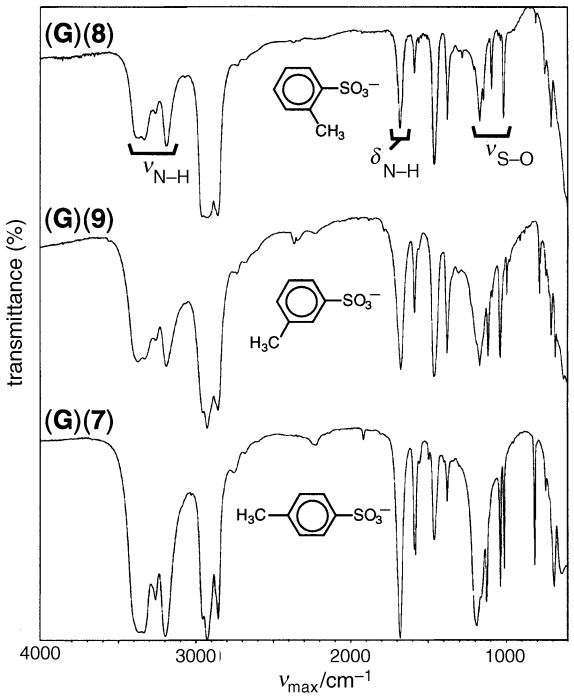

Fig. 5 Comparison of the solid-state IR spectra (Nujol mulls) of guanidinium toluenesulfonates (**G**)(**8**) (*ortho*-substituted), (**G**)(**9**) (*meta*-substituted), and (**G**)(**7**) (*para*-substituted). The structure of the n_{N-H} absorption bands, which is diagnostic of the quasihexagonal **GS** network, is essentially identical in these spectra. This argues that (**G**)(**8**), for which a single crystal structure could not be obtained, possesses a quasihexagonal hydrogen-bonding motif.

nitro groups out of the ring planes most likely arises from the need to relieve steric crowding with the *ortho* sulfonate groups and to alleviate repulsive interaction with the negatively charged sulfonate groups. A database study of *ortho*-substituted nitro groups found an average twist angle of $27 \pm 1^\circ$ for nitro groups with one substituent in the *ortho* position ($n = 392$, $n =$ number of observations).[24] When the substituent is a sulfonate group (a substantially smaller sample, $n = 7$), both steric hindrance and a negative charge are important factors, resulting in a much larger mean twist angle of $65 \pm 3^\circ$, very close to that observed in our guanidinium nitrobenzenesulfonate compounds. The database study also revealed that for nitro groups with two sterically undemanding hydrogen atoms in the positions *ortho* to the nitro group (as in the 4-, 2,4-, and 2,4,6-dinitrobenzenesulfonate compounds), a nearly coplanar arrangement with the benzene rings is favoured (average twist angle of $7.3 \pm 0.3^\circ$, $n = 270$). Steric effects clearly play a role in determining the geometry of the *ortho* nitro substituents.

The guanidinium salts of mono-substituted nitrobenzenesulfonates crystallize with structures similar to those of other

Table 2 Summary of key structural parameters and layering motifs for layered guanidinium sulfonates

compound	(G)(3)	(G)(9)	(G)(11)	(G)(12)	(G)(13)
repeat distance d ribbon, d_{rib}/Å	$b = 7.69$	$b = 7.60$	$b = 7.56$	$b = 7.59$	$b = 7.63$
repeat distance ~) ribbon, d_{rib}/Å	$c = 10.74$	$c = 8.61$	$c = 8.37$	$a = 7.24$	$a = 7.20$
HB plane	(100)	(100)	(100)	(001)	(001)
layering motif	single layer	single layer	single layer	bilayer	bilayer
interribbon dihedral angle, h_{IR}/°	153	88	86	180	180
stacking repeat distance, d_{stk}/Å	8.58	8.71	10.51	11.89	11.45

guanidinium organosulfonates, with the nitro groups influencing the crystal packings in subtle ways (Fig. 6). Guanidinium 2- and 3-nitrobenzenesulfonates (**G**)(**12**) and (**G**)(**13**) possess planar quasihexagonal hydrogen-bonded sheets ($h_{IR} = 180°$) arranged in a bilayer stacking motif (the latter contrasts with the single layer motif observed for (**G**)(**9**), the *meta* methyl substituted analogue). The planarity of these networks is unusual when compared to other guanidinium arenesulfonates with bilayer structures, which exhibit h_{IR} values of 150–165°.

Inspection of the structures of (**G**)(**12**) and (**G**)(**13**) reveals p–p stacking between arene rings in the bilayer galleries, in which the rings are laterally offset in a manner commonly observed for p–p stacks. These interactions appear to be significant, as indicated by the very short distances of 3.46 and 3.34 Å between neighbouring ring planes in (**G**)(**12**) and (**G**)(**13**), respectively. These structures differ from those of other guanidinium arenesulfonates, in which the arene rings in the bilayer galleries adopt the herringbone (edge-to-face) arrangement. The inversion symmetry within the layers results in a favourable configuration in which nitrobenzene dipoles are opposed. As in many organic crystals, the nitro groups in (**G**)(**12**) and (**G**)(**13**) do not participate in strong hydrogen bonds. While the major driving force controlling the crystal packing in both (**G**)(**12**) and (**G**)(**13**) is the hydrogen bonding within the **GS** sheets, inspection of the structures suggests that secondary C—H , O interactions[25–29] may play a role in influencing the orientations of the molecules in the van der Waals interlayer regions. Additionally, one short contact of a nitro oxygen to a guanidinium ion is present in (**G**)(**12**), with a bifurcated nitrogen oxygen acceptor forming a four-membered ring with one guanidinium NH_2 group.

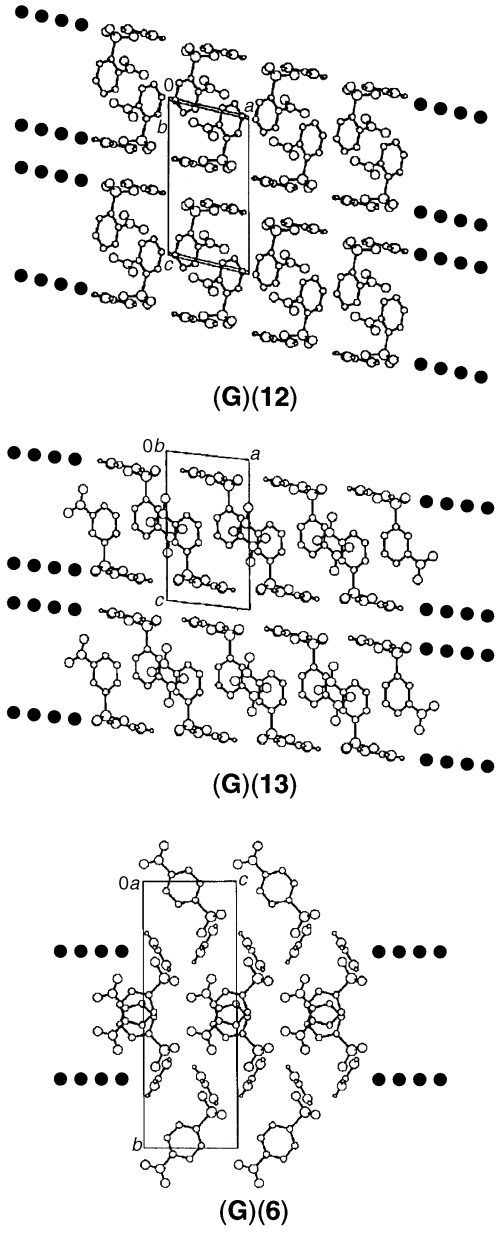

Fig. 6 Crystal structures of guanidinium 2-nitrobenzenesulfonate (**G**)(**12**), guanidinium 3-nitrobenzenesulfonate (**G**)(**13**), and guanidinium 4-nitrobenzenesulfonate (**G**)(**6**) as viewed along the hydrogen-bonded ribbon direction, which extends out of the plane of the paper. These views illustrate the segregation of the non-polar arene-containing regions and the polar hydrogen-bonding regions into bilayers for (**G**)(**12**) and (**G**)(**13**), and severely puckered interdigitated single layers for (**G**)(**6**). The filled circles denote the hydrogen-bonded quasihexagonal **GS** sheet.

The d_{rib} and d_{rib} values are nearly identical in (**G**)(**12**) and (**G**)(**13**). However, the d_{stk} values differ due to the different steric demands along the layer stacking direction imposed by the different position of the nitro groups (Table 2). We note that the bilayer structures of (**G**)(**12**) and (**G**)(**13**) differ markedly from the single layer motif found in guanidinium 4-nitrobenzenesulfonate (**G**)(**6**). This difference can be attributed to (guanidinium)N—H , O(nitro) hydrogen-bonding interactions in (**G**)(**6**), in which a nitro group extending from a **GS** sheet hydrogen bonds to two guanidinium protons on an opposing **GS** sheet. These examples illustrate that weak electrostatic interactions, steric effects, and hydrogen-bonding all contribute to the solid state packing in these salts.

Guanidinium 2,4-dinitrobenzenesulfonate (**G**)(**14**), its monohydrate (**G**)(**14**)·H_2O, and picrylsulfonate (**G**)(**15**) salts do not exhibit quasihexagonal layered **GS** sheets (Fig. 7 and 8). Rather, these compounds form complex hydrogen bonding networks that organize the hydrophobic arene-containing regions into galleries separated by two-dimensional polar regions containing the hydrogen bonding guanidinium ions, sulfonate groups and nitro groups. The major difference between the structures of (**G**)(**14**) and (**G**)(**15**) arises from the orientation of guanidinium ions with respect to the arene ring planes. Hydrogen-bonding between guanidinium protons and sulfonate and nitro acceptors is extensive in these compounds. The orientations of the guanidinium ions allow them to participate in multiple hydrogen bonds with both sulfonate and nitro acceptor sites of neighbouring anion sheets. The strongest hydrogen bonding occurs for (guanidinium) N—H , O(sulfonate) hydrogen bonds as expected, but many (guanidinium)N—H , O(nitro) C—H , O intermolecular contacts are also observed. Although weak attractive nitro , nitro intermolecular N , O contacts have been suggested to direct crystal packing in complexes of *N*,*N*-dipicrylamine,[30] this type of interaction is not present in the guanidinium nitrobenzenesulfonate salts described here. The nitro group substituents in (**G**)(**14**), (**G**)(**14**)·H_2O and (**G**)(**15**) so severely perturb the **GS** HB network that even the **GS** hydrogen-bonded ribbon motif, which is pervasive and has been observed in *all* previously determined structures of guanidinium alkane- and arene-sulfonates, is absent. However, six-membered **GS** ring motifs are present that differ from the eight-membered ring dimers in the **GS** sheets, but are similar to those found in guanidinium carboxylates and phosphates.[31,32] These structures reveal that the presence of numerous weak hydrogen bonding interactions can steer the crystal packing away from the quasihexagonal **GS** motif. A more detailed description of these complex hydrogen-bonding motifs has been reported previously.[33]

Comparison of methyl and nitro substitution

A comparison of the layering structures of the guanidinium methyl- and nitro-benzenesulfonates reveals that bilayer motifs

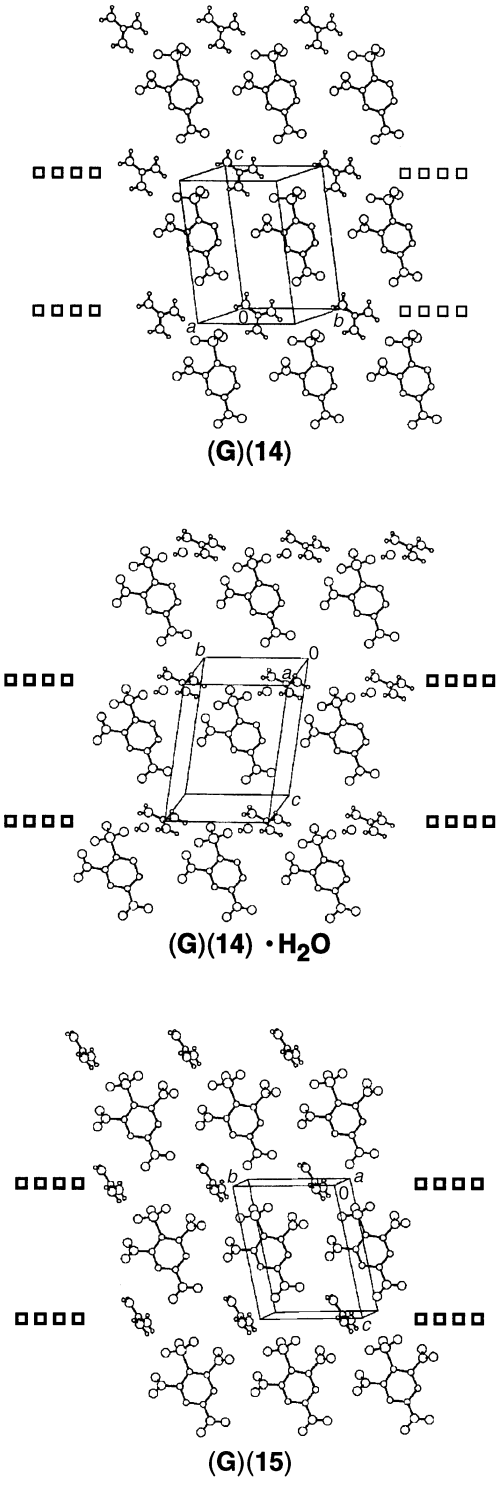

Fig. 7 Crystal structures of guanidinium 2,4-dinitrobenzenesulfonate (**G**)(**14**), guanidinium 2,4-dinitrobenzenesulfonate monohydrate (middle) (**G**)(**14**)·H_2O, and guanidinium 2,4,6-trinitrobenzenesulfonate (**G**)(**15**) as viewed normal to their (100) planes. These views illustrate the segregation, on (001) planes, of the non-polar arene-containing regions and the polar hydrogen-bonding regions (indicated by the open squares) containing the guanidinium ions, nitro and $-SO_3$ groups. The severe tilting of guanidinium ions and the presence of nitro groups in the polar region prohibit the formation of the quasihexagonal **GS** sheet. The (100) planes of (**G**)(**14**) and (**G**)(**15**) consist of arenesulfonate layers in which the arene rings lie in the plane. The arenesulfonate layers in (**G**)(**14**)·H_2O actually lie in the (102) plane. These layers are evident in the views depicted in Fig. 8.

are observed for guanidinium tosylate (**G**)(**7**) and 2- and 3-nitrobenzenesulfonates (**G**)(**12**) and (**G**)(**13**), while puckered single layer motifs are observed for guanidinium toluene-3-(**G**)(**9**), mesitylene- (**G**)(**11**), and 4-nitrobenzene-sulfonates (**G**)(**6**). The van der Waals volume of the nitro group is significantly larger than its methyl counterpart, with volumes of 23.5 and 15.3 Å^3, respectively.[34] However, the shape of the planar nitro group may provide some relief from steric crowding around the sulfonate group as it can twist out of the arene ring plane, whereas the geometry of the methyl group is more isotropic. However, twisting of the nitro group may not have a large effect, as the steric bulk of the nitro group is still larger than the methyl group. The substitution of methyl for nitro in the case of the *meta*-substituted salts (**G**)(**9**) and (**G**)(**13**) results in an unexpected change in the layering motif, with the former crystallizing in an extremely puckered single layer structure and the latter crystallizing in the bilayer motif. This is counter-intuitive as the smaller volume of **9** should make the bilayer structure more favourable for this compound. These structures reveal that steric effects are quite subtle, particularly when comparing substituents with differing substitutional position or hydrogen bonding ability. The presence of two or more nitro groups on an arenesulfonate so severely perturbs hydrogen bonding that the **GS** sheet network, so pervasive in these materials, is completely absent in compounds derived from these anions.

Conclusion

This work demonstrates that crystal packing can be controlled through use of the guanidinium-sulfonate module as a topological director of crystal packing. Guanidinium salts of benzenesulfonates containing a single methyl or nitro substituent or multiple methyl substituents crystallize with the predicted quasihexagonal **GS** network, with layers assembling into either bilayer or single layer motifs. The robustness and prevalence of the **GS** network suggests that this module can be used in the design and synthesis of new crystalline materials. Its two-dimensional nature reduces crystal engineering to the last remaining dimension. However, unanticipated differences in layering motif, *i.e.* bilayer *versus* single layer packing, for analogous methyl *versus* nitro substituted benzenesulfonate salts shows that subtle steric and hydrogen-bonding effects can have a dramatic effect in determining crystal packing in the third dimension. In the cases of multiple substitution of nitro groups, the quasihexagonal HB sheets and layering structures are completely disrupted in order to form multiple weak hydrogen bonds to nitro groups. These studies illustrate that even if robust modules are employed, the presence of ancillary intermolecular interactions can limit the predictability of the entire 3D structure. However, we anticipate that restricting ancillary residues to galleries within the robust 2D HB networks, thereby limiting the degrees of freedom available for crystal packing, will facilitate computational predictions of these structures.

Experimental

Materials

Guanidine chloride and guanidine carbonate were purchased from Aldrich Chemical Co. All other starting materials were purchased from the companies indicated and used as received. Spectroscopic-grade solvents and/or deionized water were used for all crystallizations.

Characterization

Melting points were determined by differential scanning calorimetry (DSC) with a Mettler FP80/FP84 system (100 mV, 1 °C min^{-1}). Solid-state IR spectra were recorded on a Nicolet

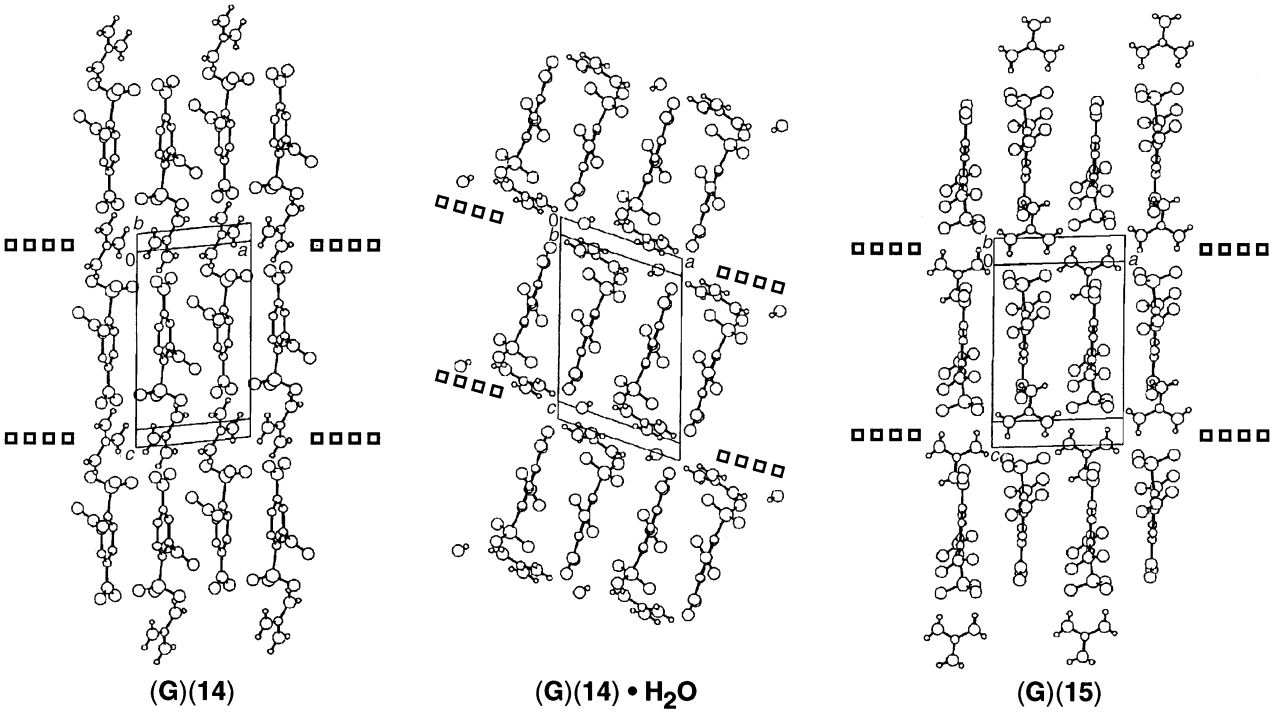

Fig. 8 Crystal structures of guanidinium 2,4-dinitrobenzenesulfonate (**G**)(**14**), guanidinium 2,4-dinitrobenzenesulfonate monohydrate (**G**)(**14**)·H_2O, and guanidinium 2,4,6-trinitrobenzenesulfonate (**G**)(**15**) as viewed normal to their (010) planes. These views illustrate the segregation, on (001) planes, of the non-polar arene-containing regions and the polar hydrogen-bonding regions (indicated by the open squares) containing the guanidinium ions, nitro and $-SO_3$ groups. The (100) planes of (**G**)(**14**) and (**G**)(**15**) consist of arenesulfonate layers in which the arene rings lie in the plane. The arenesulfonate layers in (**G**)(**14**)·H_2O actually lie in the (102) plane. Because of its severe tilt, the guanidinium cation bridges these layers by hydrogen bonding in all three compounds, resulting in a three-dimensional hydrogen-bonding network.

510M spectrometer (4 cm^{-1} resolution) as Nujol mulls. ^1H NMR spectra were recorded on an IBM NR200AF spectrometer (200MHz) in $(CD_3)_2SO$ unless stated otherwise (Cambridge Isotope Laboratories) relative to internal standard $SiMe_4$; *J* in Hz. Experimental details of the X-ray structural determinations are given in Table 1, and atomic coordinates are available as supplementary material or at our World Wide Web site (http://www.cems.umn.edu/research/ward). Structures (**G**)(**3**), (**G**)(**9**), (**G**)(**13**), (**G**)(**14**), (**G**)(**14**)·H_2O and (**G**)(**15**) were determined using an Enraf-Nonius CAD4 diffractometer with graphite monochromated Mo-Ka radiation at l 0.71069 Å. Structures (**G**)(**11**) and (**G**)(**12**) were determined using a Siemens SMART system diffractometer with graphite monochromated Mo-Ka radiation at l 0.71069 Å. All data were collected at room temp. (24 °C).

Atomic coordinates, thermal parameters, and bond lengths and angles have been deposited at the Cambridge Crystallographic Data Centre (CCDC). See Information for Authors, *J. Mater. Chem.*, 1997, Issue 1. Any request to the CCDC for this material should quote the full literature citation and the reference number 1145/37.

Guanidinium toluene-2-sulfonate acetonitrile solvate, $[C(NH_2)_3]^+$ 2-$CH_3(C_6H_4)SO_3^-\cdot CH_3CN$, (G)(8)·MeCN

This phase was recrystallized as colourless plates from a 1:1 methanol–acetonitrile solution containing equimolar quantities of guanidine hydrochloride and toluene-2-sulfonic acid (Aldrich). The following characterization was performed immediately after removal of the crystals from solution. DSC 30–52 °C (broad endotherm, loss MeCN), mp 222–224 °C; n/cm^{-1} 3363 (s), 3330 (s), 3255 (m), 3190 (s), 2252 (m, sharp), 1677 (s), 1582 (m), 1463 (s), 1378 (m), 1283 (w), 1208 (s), 1187 (s), 1171 (s), 1144 (s), 1094 (s), 1050 (m), 1038 (m), 1017 (s), 918 (vw), 808 (w), 768 (m), 741 (m), 708 (s), 614 (s); d 7.73 (~d, 1 H, *ortho* to SO_3^-), 7.21–7.12 (m, 3 H, *meta*/*para* to SO_3^-), 6.95 {s, 6 H, $[C(NH_2)_3]$}, 2.52 (s, 3 H, Ar-CH_3), 2.08 (s, 3 H, CH_3CN). The presence of acetonitrile is confirmed by IR (n_{CN} at 2252 cm^{-1}) and by observation of its methyl protons in the ^1H NMR spectrum at 2.08 ppm, as well as a broad desolvation endotherm in the DSC. The crystals desolvate soon after their removal from solution, resulting in an opaque solid having an IR spectrum identical to (**G**)(**8**).

Guanidinium toluene-2-sulfonate, $[C(NH_2)_3]^+$ 2-$CH_3(C_6H_4)SO_3^-$, (G)(8)

This phase was isolated from a 1:1 methanol–acetonitrile solution containing equimolar quantities of guanidine hydrochloride and toluene-2-sulfonic acid (Aldrich). This compound formed as an opaque solid on the sides of the crystallization vessel or after desolvation of solvated crystals (**G**)(**8**)·MeCN. Attempts to isolate single crystals of (**G**)(**8**) from solution were difficult, but clear thin needles of unsolvated (**G**)(**8**) were isolated together with opaque solid (presumably, desolvated (**G**)(**8**)·H_2O or (**G**)(**8**)·EtOH) from 20% aqueous ethanol. However, these needles were not large enough for single crystal X-ray diffraction. DSC mp 220–222 °C; n/cm^{-1} 3365 (s), 3332 (s), 3259 (m), 3186 (s), 1683 (s), 1588 (m), 1463 (s), 1378 (s), 1302 (w), 1281 (w), 1208 (m), 1169 (s), 1146 (s), 1094 (m), 1052 (vw), 1036 (vw), 1017 (s), 808 (w), 751 (m), 708 (s); d 7.73 (~d, 1 H, *ortho* to SO_3^-), 7.21–7.12 (m, 3 H, *meta*/*para* to SO_3^-), 6.95 {s, 6 H, $[C(NH_2)_3]$}, 2.52 (s, 3 H, Ar-CH_3).

Guanidinium toluene-3-sulfonate, $[C(NH_2)_3]^+$ 3-$CH_3(C_6H_4)SO_3^-$, (G)(9)

This phase was crystallized from methanol or 10% aqueous acetonitrile solutions containing equimolar quantities of guanidine hydrochloride and toluene-3-sulfonic acid monohydrate (Lancaster) or from aqueous solutions containing 1:2 molar quantities of guanidine carbonate and toluene-3-sulfonic acid

monohydrate as colourless needles: DSC with concurrent visual observation 152–156 (slightly broad endotherm, crystals fracture, turn somewhat cloudy), mp 215–216 °C; visual observation of single crystals on a Fisher–Johns hot stage: 155–160 °C: very slight clouding, but crystal remained somewhat clear, possibly melting and resolidifying; 218–219 °C: melting; n/cm^{-1} 3371 (s), 3328 (s), 3257 (m-s), 3190 (s), 1677 (s), 1586 (m), 1463 (s), 1378 (s), 1304 (w), 1225 (m, sh), 1194 (s, sh), 1169 (s), 1115 (s), 1090 (m), 1038 (s), 996 (m), 783 (m), 741 (w), 708 (m), 681 (s), 627 (s); d 7.43 (~d, 2 H, Ar-*H ortho* to SO_3^-), 7.22–7.15 (m, 2 H, *J* 7.9, Ar-*H meta* and *para* to SO_3^-), 6.96 {s, 6 H, $[C(NH_2)_3]^+$}, 2.32 (s, 3 H, Ar-CH_3). The X-ray crystal structure of this compound was solved.

Guanidinium 2,4-dimethylbenzenesulfonate $[C(NH_2)_3]^+$ 2,4-$(CH_3)_2(C_6H_3)SO_3^-$, (G)(10)

This phase was crystallized from 3:1 methanol–toluene solution containing equimolar quantities of guanidine hydrochloride and sodium 2,4-dimethylbenzenesulfonate (Kodak) as colourless needles; DSC mp 281 °C; n/cm^{-1} 3373 (s), 3330 (s), 3263 (m), 3188 (s), 1677 (s), 1588 (m), 1463 (s), 1378 (s), 1189 (m), 1158 (s), 1092 (m), 1017 (s), 822 (w), 816 (w), 745 (w), 726 (w), 685 (m); d 7.60 (d, 1 H, $J = 7.6$), 6.95 with 6.92 side peak {s, 8 H, $[C(NH_2)_3]^+$, Ar-*H ortho* to SO_3^-}, 2.48 (s, 3 H, Ar-CH_3), 2.25 (s, 3 H, Ar-CH_3). An attempt was made to solve the X-ray crystal structure, but refinement was not successful. The structure determination was not pursued further.

Guanidinium mesitylenesulfonate (guanidinium 2,4,6-trimethylbenzenesulfonate), $[C(NH_2)_3]^+$ 2,4,6-$(CH_3)_3(C_6H_2)SO_3^-$, (G)(11)

This phase was crystallized from methanol or 30% aqueous acetonitrile solutions containing equimolar quantities of guanidine hydrochloride and mesitylenesulfonic acid dihydrate (Aldrich) or from aqueous or methanol solutions containing 1:2 molar quantities of guanidine carbonate and mesitylenesulfonic acid dihydrate as aggregates of colourless rectangular, flat plates: DSC mp 270–300 (decomp.)°C; n/cm^{-1} 3375 (s), 3323 (s), 3259 (m-s), 3186 (s), 1675 (s), 1605 (w), 1586 (m), 1569 (w), 1461 (s), 1378 (s), 1252 (w), 1191 (m), 1183 (m), 1158 (s), 1092 (s), 1013 (s), 841 (m), 743 (m), 689 (s); d 6.97 {s, 6 H, $[C(NH_2)_3]^+$}, 6.77 (s, 2 H, arene ring H), 2.50 (s, ~6 H, 2,6-CH_3, overlaps with $(CH_3)_2SO$ solvent peak), 2.18 (s, 3 H, 4-CH_3); d (D_2O) 7.05 (s, 2 H, arene ring H), 4.91 {s, $[C(NH_2)_3]^+$, overlaps with H_2O solvent impurity peak}, 2.57 (s, 6 H, 2,6-CH_3), 2.29 (s, 3 H, 4-CH_3). The X-ray crystal structure of this compound was solved.

Guanidinium 2-nitrobenzenesulfonate, $[C(NH_2)_3]^+$ 2-$NO_2(C_6H_4)SO_3^-$, (G)(12)

This phase was crystallized from methanol solution containing equimolar quantities of guanidine hydrochloride and 2-nitrobenzenesulfonic acid (Pfaltz and Bauer) as colourless thick hexagonal plates and wide needles or from methanol–toluene solution as colourless needles: DSC endotherm 117–118, mp 129–135 °C; n/cm^{-1} 3406 (s), 3381 (s), 3284 (m), 3255 (m), 3213 (s), 1679 (s), 1598 (w), 1578 (m), 1538 (s, $n_{N\text{-}O}$ asym), 1463 (s, Nujol), 1378 (s, Nujol, overlapping with $n_{N\text{-}O}$ sym), 1302 (w), 1270 (w), 1208 (s), 1171 (m), 1146 (m), 1079 (m), 1042 (w), 1025 (s), 857 (w-m), 776 (m), 743 (m), 733 (m), 662 (s), 614 (s); d 7.85 (~d, 1 H, 6-Ar-*H*), 7.63–7.55 (m, 3 H, 3,4,5-Ar-*H*), 6.94 {s, 6 H, $[C(NH_2)_3]^+$}; d (D_2O) d 8.02–8.00 (m, 1 H, 6-Ar-*H*), 7.77–7.71 (m, 3 H, 3,4,5-Ar-*H*), 4.80 {s, ~10 H, $[C(NH_2)_3]^+$, also contains HDO peak}. The X-ray crystal structure of this compound was solved.

Guanidinium 2-nitrobenzenesulfonate hydrate, $[C(NH_2)_3]^+$ 2-$NO_2(C_6H_4)SO_3^- \cdot H_2O$, (G)(12)·x$H_2O$

This phase was crystallized from 10% aqueous acetonitrile solution containing equimolar quantities of guanidine hydrochloride and 2-nitrobenzenesulfonic acid (Pfaltz and Bauer) or from aqueous or 10% aqueous methanol solutions containing 1:2 molar quantities of guanidine carbonate and 2-nitrobenzenesulfonic acid as colourless needles: DSC endotherms: 72–76 (br), 90–95 (br), mp 134–136 °C; n/cm^{-1} 3656 (m), 3558 (m), 3440 (sh, s), 3367 (s), 3274 (s), 3205 (s), 3095 (m), 1675 (s), 1613 (w), 1596 (w), 1582 (m), 1540 (s, $n_{N\text{-}O}$ asym), 1530 (s, $n_{N\text{-}O}$ asym), 1465 (s), 1374 (s, $n_{N\text{-}O}$ sym), 1364 (s, $n_{N\text{-}O}$ sym), 1300 (w), 1214 (s), 1164 (m), 1142 (s), 1079 (s), 1040 (m), 1025 (s), 855 (m), 780 (m), 743 (s), 733 (s), 702 (m), 664 (s), 646 (s), 614 (s), 581 (s); d 7.85 (~d, 1 H, 6-Ar-*H*), 7.60–7.55 (m, 3 H, 3,4,5-Ar-*H*), 6.93 {s, 6 H, $[C(NH_2)_3]^+$}, 3.41 (s, H_2O, ~5 H, hydrate and exchange with water in Me_2SO). The stoichiometric amount of hydrated water in the crystal was not determined. However, this salt may be a dihydrate, as indicated by the two broad endotherms in the DSC. The integration of the water peak in the NMR to a value corresponding to nearly four hydrogens also suggests that the complex may be a dihydrate. The sharp IR $n_{O\text{-}H}$ at high wavenumber positions indicate that the water is not strongly associated by hydrogen bonding in the lattice. The existence of split IR $n_{N\text{-}O}$ bands at 1540/1530 cm^{-1} and 1374/1364 cm^{-1} suggests two different solid-state environments for the nitro group and possibly two ion pairs in the asymmetric unit.

Guanidinium 3-nitrobenzenesulfonate, $[C(NH_2)_3]^+$ 3-$NO_2(C_6H_4)SO_3^-$, (G)(13)

This phase was crystallized from 25% aqueous acetonitrile or 3:3:1 methanol–ethyl acetate–water solutions containing equimolar quantities of guanidine hydrochloride and sodium 3-nitrobenzenesulfonate (Kodak) as light-yellow elongated diamonds/parallelograms: DSC endotherm 178–180, mp 184–187 °C; visual observation of a single crystal on a Fisher–Johns hot stage showed no obvious change at 180 °C and melting at 185–190 °C; n/cm^{-1} 3400 (s), 3371 (s), 3249 (m), 3207 (s), 3105 (w), 1673 (s), 1580 (m), 1573 (m), 1532 (s, $n_{N\text{-}O}$ asym), 1465 (s, Nujol), 1378 (s, Nujol), 1356 (s, $n_{N\text{-}O}$ sym), 1277 (w), 1208 (s), 1150 (m), 1096 (m), 1079 (m), 1038 (m-s), 1001 (w), 934 (w), 907 (w), 882 (w), 812 (m), 762 (m), 737 (m), 671 (s); d 8.34 (m, 1 H, 2-Ar-*H*), 8.22 (d, 1 H, *J* 9.1, 6-Ar-*H*), 8.03 (d, 1 H, J 7.7, 4-Ar-*H*), 7.67 (t, 1 H, *J* 7.9, 5-Ar-*H*), 6.93 {s, 6 H, $[C(NH_2)_3]^+$}. The X-ray crystal structure of this compound was solved.

Guanidinium 2,4-dinitrobenzenesulfonate, $[C(NH_2)_3]^+$ 2,4-$(NO_2)_2(C_6H_3)SO_3^-$, (G)(14)

This phase was crystallized from 1:1 methanol–ethyl acetate solution containing equimolar quantities of guanidine hydrochloride and 2,4-dinitrobenzenesulfonic acid (Eastman) as hard, light tan needles or from 10% aqueous acetonitrile solution as opaque cream-coloured powder. The opaque material is probably a dehydrated form of (G)(14)·H_2O, as dehydration of (G)(14)·H_2O yields an identical solid based on IR spectroscopy. DSC mp 176 °C; n/cm^{-1} 3477, 3433, 3365, 3272, 3199, 3095, 1675, 1663, 1605, 1551 (s, $n_{N\text{-}O}$ asym), 1542, 1465, 1378, 1368, 1356 (s, $n_{N\text{-}O}$ sym), 1227, 1136, 1119, 1069, 1028, 906, 849, 834, 750, 739, 724, 662, 635; d 8.58 (d, 1 H, *J* 2.3), 8.42 (dd, 1 H, J_1 8.6, J_2 2.3), 8.11 (d, 1 H, *J* 8.6), 6.92 (s, 6 H). The X-ray crystal structure of this compound was solved.

Guanidinium 2,4-dinitrobenzenesulfonate monohydrate, $[C(NH_2)_3]^+$ 2,4-$(NO_2)_2(C_6H_3)SO_3^- \cdot H_2O$, (G)(14)·$H_2O$

This phase was crystallized from aqueous or 10% aqueous acetonitrile solutions containing equimolar quantities of

guanidine hydrochloride and 2,4-dinitrobenzenesulfonic acid (Eastman) as light tan parallelograms/plates: DSC endotherm 60–69 (br, determined to be loss of H_2O by comparison of IR spectra), mp 173–175 °C. Note that the dehydration endotherm position may vary depending upon sample, but occurs at 50–90° and within a 10–15° range; n/cm^{-1} 3587, 3494, 3452, 3404, 3365, 3265, 3203, 3107, 3099, 1675, 1636, 1605, 1574, 1547 (s, $n_{N\text{-}O}$ asym), 1536, 1465, 1378, 1364 (s, $n_{N\text{-}O}$ sym), 1312, 1239, 1227, 1154, 1138, 1119, 1067, 1032, 974, 920, 905, 859, 837, 754, 745, 718, 641, 594; d 8.57 (d, 1 H, *J* 2.2), 8.42 (dd, 1 H, J_1 8.6, J_2 2.3), 8.10 (d, 1 H, *J* 8.6), 6.92 (s, 6 H), 3.37 [s, ~3 H: 2 H from hydrated water of the crystal, ~1 H from H_2O impurity in $(CD_3)_2SO$]. Crystals of (**G**)(**12**)·H_2O are stable for days to weeks after removal from solution, but eventually dehydrate, as suggested by a loss of crystal transparency and confirmed by IR spectroscopy. The low temperature of dehydration characterized by DSC suggests that the water molecules are loosely bound in the lattice, as also suggested by the high wavenumber $n_{O\text{-}H}$ IR band at 3587 cm^{-1}. The X-ray crystal structure of this compound was solved. No hydrogens were refined in the structure determination except one water proton, H10, which was identified on the difference map and refined. The other water proton could not be located on the difference map and was left out.

Guanidinium picrylsulfonate (guanidinium 2,4,6-trinitrobenzenesulfonate), $[C(NH_2)_3]^+$ $2,4,6\text{-}(NO_2)_3(C_6H_2)SO_3^-$, (G)(15)

This phase was crystallized from a methanol–toluene solution containing equimolar quantities of guanidine hydrochloride and picrylsulfonic acid trihydrate (Kodak) as very high quality light-yellow, thick plates with well-developed faces: DSC exotherms 230–233, 239–241 °C (decomp.); visual observation of single crystals on a Fisher–Johns hot stage confirmed the decomposition: crystals begin to turn brown at 225 °C and eventually turn black with bubbling occurring from 236–240 °C; n/cm^{-1} 3492 (m), 3456 (m-s), 3377 (m), 3290 (m), 3213 (w), 3095 (w), 3083 (m), 1661 (s, sl br), 1609 (m), 1559 (s, $n_{N\text{-}O}$ asym), 1546 (s, $n_{N\text{-}O}$ asym), 1465 (s), 1378 (s, possibly $n_{N\text{-}O}$ sym), 1356 (s, $n_{N\text{-}O}$ sym), 1252 (s), 1233 (s), 1131 (m), 1073 (m), 1030 (m), 974 (w), 926 (w), 907 (w), 753 (m), 735 (m), 724 (m), 631 (m); d 8.85 (s, 2 H, Ar-*H*), 6.90 {s, 6H, $[C(NH_2)_3]^+$}. The X-ray crystal structure of this compound was solved.

Guanidinium 4-nitrotoluene-2-sulfonate, $[C(NH_2)_3]^+$ $4\text{-}(NO_2)\text{-}2\text{-}(CH_3)\text{-}(C_6H_3)SO_3^-$, (G)(16)

This phase was crystallized from methanol or 10% aqueous acetonitrile solutions containing equimolar quantities of guanidine hydrochloride and 4-nitrotoluene-2-sulfonic acid dihydrate (Pfaltz and Bauer) or from aqueous or methanol solutions containing 1:2 molar quantities of guanidine carbonate and 4-nitrotoluene-2-sulfonic acid dihydrate as very fine colourless to light tan aggregates of needles. An opaque solid was also isolated on the sides of the crystallization vessels, suggesting that the solid may be a desolvated solvate form. The IR spectrum of the opaque solid matched that of the colourless needles. DSC mp 249 °C; n/cm^{-1} 3469 (m), 3369 (s), 3340 (s, sh), 3267 (m), 3193 (s), 1673 (m), 1585 (m), 1519 (s, $n_{N\text{-}O}$ asym), 1465 (m), 1380 (m), 1355 (s, $n_{N\text{-}O}$ sym), 1308 (w), 1268 (w), 1229 (s), 1198 (m), 1150 (m), 1079 (s), 1028 (s), 922 (w), 915 (w), 895 (w), 833 (w), 801 (w), 741 (m), 720 (m), 704 (m), 617 (s); d 8.51 (~d, 1 H, 3-Ar-*H*), 8.09 (dd, 1 H, 5-Ar-*H*), 7.47 (d, 1 H, *J* 8.4, 6-Ar-*H*), 6.94 {s, 6 H, $[C(NH_2)_3]^+$}, 2.66 (s, 3 H, Ar-CH_3).

The authors gratefully acknowledge the National Science Foundation and the Office of Naval Research for financial support, and Professor J. Doyle Britton and Dr Victor Young for crystallographic services.

References

1 J.-M. Lehn, M. Mascal, A. DeCian and J. J. Fisher, *J. Chem. Soc., Perkin Trans. 2*, 1992, 461.
2 E. Fan, L. Yang, S. J. Geib, T. C. Stoner, M. D. Hopkins and A. D. Hamilton, *J. Chem. Soc., Chem. Commun*., 1995, 1251.
3 J. C. MacDonald and G. M. Whitesides, *Chem. Rev*., 1994, **94**, 2383.
4 J. A. Zerkowski, J. C. MacDonald, C. T. Seto, D. A. Wierda and G. M. Whitesides, *J. Am. Chem. Soc*., 1994, **116**, 4305.
5 J.-M. Lehn, M. Mascal, A. DeCian and J. J. Fisher, *J. Chem. Soc., Chem. Commun*., 1990, 479.
6 X. Wang, M. Simard and J. D. Wuest, *J. Am. Chem. Soc*., 1994, **116**, 12119.
7 M. Simard, D. Su and J. D. Wuest, *J. Am. Chem. Soc*., 1991, **113**, 4696.
8 O. Ermer and L. A. Lindenberg, *Helv. Chim. Acta*, 1991, **74**, 825.
9 O. Ermer, *J. Am. Chem. Soc*., 1988, **111**, 3747.
10 M. J. Zaworotko, *Chem. Soc. Rev*., 1994, 283.
11 V. A. Russell, C. C. Evans, W. Li and M. D. Ward, *Science*, in press.
12 V. A. Russell and M. D. Ward, *Chem. Mater*., 1996, **8**, 1654.
13 G. R. Desiraju, *Angew. Chem., Int. Ed. Engl*., 1995, **34**, 2311.
14 V. A. Russell, M. C. Etter and M. D. Ward, *J. Am. Chem. Soc*., 1994, **116**, 1941.
15 V. A. Russell, M. C. Etter and M. D. Ward, *Chem. Mater*., 1994, **6**, 1206.
16 V. A. Russell and M. D. Ward, *Acta Crystallogr. Sect. B*, 1996, **52**, 209.
17 V. A. Russell and M. D. Ward, Proceedings of the NATO Advanced Research Workshop on Modular Chemistry, September 9–12, Estes Park, Colorado, in press.
18 M. C. Etter, *J. Phys. Chem*., 1991, **95**, 4601.
19 M. E. Thompson, *Chem. Mater*., 1994, **6**, 1168.
20 K. P. Reis, V. K. Joshi and M. E. Thompson, *J. Catal*., 1996, **161**, 62.
21 G. Cao and T. E. Mallouk, *J. Solid State Chem*., 1991, **94**, 59.
22 F. H. Allen, O. Kennard, D. G. Watson, L. Brammer, A. G. Orpen and R. Taylor, *J. Chem. Soc., Perkin Trans. 2*, 1987, S1.
23 G. R. Desiraju, *Crystal Engineering: The Design of Organic Solids*, Elsevier, New York, 1989, p. 92ff.
24 D. J. A. De Ridder and H. Schenk, *Acta Crystallogr. Sect. B*, 1995, **51**, 221.
25 G. R. Desiraju, *Acc. Chem. Res*., 1996, **29**, 441.
26 G. R. Desiraju, *Acc. Chem. Res*., 1991, **24**, 290.
27 J. A. R. P. Sarma and G. R. Desiraju, *Acc. Chem. Res*., 1986, **19**, 222.
28 J. A. R. P. Sarma and G. R. Desiraju, *J. Chem. Soc., Perkin Trans. 2*, 1987, 1195.
29 Z. Berkovitch-Yellin and L. Leiserowitz, *Acta Crystallogr. Sect. B*, 1984, **40**, 159.
30 K. Wozniak, H. He, J. Klinowski, W. Jones and E. Grech, *J. Phys. Chem*., 1994, **98**, 13755.
31 D. M. Salunke and M. Vijayan, *Int. J. Peptide Protein Res*., 1981, **18**, 348.
32 Y. Yokomori and D. J. Hodgson, *Int. J. Peptide Protein Res*., 1988, **31**, 289.
33 V. A. Russell, PhD Thesis, University of Minnesota, 1995.
34 A. Gavezzotti, in *Structure correlation* ed. H.-B. Burgi and J. D. Dunitz, VCH, New York, 1994, vol. 2, ch. 12. The van der Waals volumes have also been reported as 13.67 and 16.8 (for nitro attached to carbon atom) cm^3 mol^{-1} for methyl and nitro groups, respectively: A. Bondi, *J. Phys. Chem*., 1964, **68**, 441.

Paper 7/00023E; *Received* 2*nd January*, 1997